Proceedings of the ASME 2011 30th International Conference on Ocean, Offshore and Arctic Engineering
OMAE2011
June 19-24, 2011, Rotterdam, The Netherlands

OMAE2011-49116

A GENERIC OPTIMIZATION ALGORITHM FOR THE ALLOCATION OF DP ACTUATORS

Dr. ir. E.F.G. van Daalen
Maritime Research Institute Netherlands (MARIN)
Wageningen, The Netherlands

J.L. Cozijn
Maritime Research Institute Netherlands (MARIN)
Wageningen, The Netherlands

C. Loussouarn
Ecole Polytechnique
Palaiseau, France

Prof. Dr. P.W. Hemker
Centrum Wiskunde & Informatica (CWI)
Amsterdam, The Netherlands

ABSTRACT

In this paper we present a generic optimization algorithm for the allocation of dynamic positioning actuators, such as azimuthing thrusters and fixed thrusters. The algorithm is based on the well-known Lagrange multipliers method. In the present approach the Lagrangian functional represents not only the cost function (the total power delivered by all actuators), but also all constraints related to thruster saturation and forbidden zones for azimuthing thrusters.

In the presented approach the application of the Lagrange multipliers method leads to a nonlinear set of equations, because an exact expression for the total power is applied and the actuator limitations are accounted for in an implicit manner, by means of nonlinear constraints. It is solved iteratively with the Newton-Raphson method and a step by step implementation of the constraints related to the actuator limitations.

In addition, the results from the non-linear solution method were compared with the results from a simplified set of linear equations, based on an approximate (quadratic) expression for the thruster power. The non-linear solution was more accurate, while requiring only a slightly higher computational effort.

An example is shown for a thruster configuration with 8 azimuthing thrusters, typical for a DP semi-submersible. The results show that the optimization algorithm is very stable and efficient.

Finally, some options for improvements and future enhancements – such as including thruster-thruster and thruster-hull interactions and the effects of current – are discussed.

INTRODUCTION

With the offshore industry moving to ever deeper waters, more and more vessels are equipped with dynamic positioning (DP) systems. On a DP vessel a feedback system controls the thrusters to keep the vessel in a fixed position, thus eliminating the need for mooring lines. The components in a DP system are described in more detail below.

Components in a DP system

The DP system on board a vessel contains several different hardware and software components. These components are shown in the schematic overview in Figure 1. The main components of the DP system are briefly described below. More detailed explanations can be found in [1], [2] and [3].

- ***Position Measurement***: The position of the control point (CP) on the vessel is measured using e.g. GPS or an acoustic position reference system.
- ***Extended Kalman Filter (EKF)***: The EKF determines the low frequency motions and velocities of the vessel. The purpose of the filter is to avoid thruster response to wave frequency vessel motions.
- ***Position Error***: The estimated low frequency position and velocity are compared to the position and velocity of the reference point (RP). The resulting position error is forwarded to the Controller.

- ***Controller***: Based on the horizontal offset from the RP and the velocity of the vessel, the Controller determines the required total surge and sway forces and yaw moment.
- ***Allocation Algorithm***: The Allocation Algorithm distributes the required total forces and moment over the available actuators such that the allocated power is minimized. The allocation algorithm (marked red in Figure 1) is the component of the DP system discussed in this paper.
- ***Thrusters***: The azimuth angles and RPMs are set, based on the output of the Allocation Algorithm. The generated total forces and moment will move the vessel CP towards the RP position.

It is noted that in practical applications the response of the thrusters is limited in terms of rate of turn, as well as rate of change in RPM. This may cause differences between the total thrust requested for by the controller and the total thrust generated by the actuators, especially in relatively severe environments, close to the limitations of the vessel's stationkeeping capabilities.

Furthermore, the effective force delivered by the thrusters may be smaller than the nominal (bollard pull) thrust value. This difference is caused by thruster-interaction (or thrust degradation) effects. The following thruster-interaction effects are mentioned:

- Thruster-hull interaction
- Thruster-thruster interaction
- Thruster-current interaction

Thruster allocation

The present paper focuses on the Allocation Algorithm. In general, there will be more variables describing the thruster settings (azimuth angle, RPM) than equations to solve (required forces and moment). The over-determined set of equations is solved in such a way to minimize the allocated power. However, the resulting optimization problem is relatively complex, for the following reasons:

- The relations between RPM, generated thrust and consumed power are non-linear.
- The thrust generated by a thruster is limited ('saturation').
- Certain orientations of an azimuthing thruster may not be allowed. These 'forbidden zones' may be defined to avoid excessive thruster-interaction losses, or to protect sensitive equipment placed under the vessel hull (e.g. hydrophones or cables).

OPTIMIZATION OF THRUSTER ALLOCATION

Introduction and definitions

We consider a vessel with N azimuthing thrusters (other types of actuators will be considered later on). Each azimuthing thruster i is characterized by the following thruster attributes:

- The position (x_i, y_i) with respect to the reference point G.
- The maximum thrust $T_{\max,i}$
- The maximum power $P_{\max,i}$

Each thruster can rotate about its vertical axis. The azimuth (angle) of thruster i is denoted by α_i, its thrust by T_i and its state is defined by the allocated surge force and sway force, combined in the state vector:

$$\vec{F}_i = (F_{x,i}, F_{y,i})^T \tag{1}$$

The contribution to the yaw moment about G is

$$M_{z,i} = x_i F_{y,i} - y_i F_{x,i} \tag{2}$$

The thrust T_i and azimuth α_i are calculated from $F_{x,i}$ and $F_{y,i}$ as follows:

$$T_i = \left\|\vec{F}_i\right\| = \sqrt{F_{x,i}^2 + F_{y,i}^2} \tag{3a}$$
$$\alpha_i = \arctan(F_{y,i} / F_{x,i}) \tag{3b}$$

Note that some angles may be prohibited: for instance, if one thruster is in the stream of another, the efficiency will drop. In certain cases, we will thus have to define a "forbidden zone" for the azimuth.

The power of thruster i is given by:

$$P_i^{(m)} = c_i T_i^m \quad \text{or} \quad P_i^{(m)} = c_i (F_{x,i}^2 + F_{y,i}^2)^{m/2} \tag{4}$$

The exact formulation for the thruster power (in bollard pull conditions) is obtained for $m = 3/2$, but this leads to a system of non-linear equations, whereas the choice $m = 2$ gives a set of linear equations which is easier to solve.

The coefficient c_i is calculated by substitution of the maximum values of the thrust and the power for $m = 3/2$:

$$c_i = \frac{P_{\max,i}}{T_{\max,i}^{3/2}} \tag{5}$$

We can then describe the system of thrusters with the global state vector

$$\vec{F} \equiv (F_{x,1}, F_{y,1}, F_{x,2}, F_{y,2}, \ldots, F_{x,N}, F_{y,N})^T \tag{6}$$

and define the total surge force, the total sway force and the total yaw moment by summation over all thrusters:

$$F_{x,\text{tot}} \equiv \sum_{i=1}^{N} F_{x,i} \;,\; F_{y,\text{tot}} \equiv \sum_{i=1}^{N} F_{y,i} \;,\; M_{z,\text{tot}} \equiv \sum_{i=1}^{N} M_{z,i} \tag{7}$$

The total power of the thruster configuration is calculated by summation of the power of the individual thrusters:

$$P_{\text{tot}}^{(m)} \equiv \sum_{i=1}^{N} P_i^{(m)} \tag{8}$$

Optimization of allocation – minimization of power

Our aim is to optimize the energy consumed by the thrusters: we search the state vector $\vec{F}$ that minimizes the object function $P_{\text{tot}}^{(m)}$ under the following set of constraints:

- The total surge and sway forces and the total yaw moment have to match the required values:

$$R_x(\vec{F}) \equiv F_{x,\text{req}} - F_{x,\text{tot}} = 0 \tag{9a}$$

$$R_y(\vec{F}) \equiv F_{y,\text{req}} - F_{y,\text{tot}} = 0 \tag{9b}$$

$$R_z(\vec{F}) \equiv M_{z,\text{req}} - M_{z,\text{tot}} = 0 \tag{9c}$$

- The thrust is limited by the maximum thrust:

$$M_i(\vec{F}) \equiv T_{\max,i}^2 - (F_{x,i}^2 + F_{y,i}^2) \geq 0 \quad i = 1, 2, \ldots, N \tag{10}$$

  If the thrust of thruster i reaches the maximum value, we will say that the thruster is 'saturated'.

- Finally we may have constraints on the azimuth: for each thruster, we define a forbidden zone, of width $2\Delta\alpha_i$ and direction $\alpha_{0,i}$, where the azimuth is not allowed.

Approximate solution without constraints

First we apply the Lagrange multipliers method to the approximate problem with $m = 2$ without any constraints on thrust and azimuth. The Lagrangian of our minimization problem is composed of the total power (8) and the three constraints (9a-c):

$$\Lambda^{(2)}(\vec{F}, \vec{\rho}) \equiv P_{\text{tot}}^{(2)}(\vec{F}) - \vec{\rho} \cdot \vec{R}(\vec{F}) \tag{11}$$

At an optimum, the gradient of Lagrangian must vanish:

$$\nabla_{\vec{F}} \Lambda^{(2)} = \vec{0} \quad \text{and} \quad \nabla_{\vec{\rho}} \Lambda^{(2)} = \vec{0} \tag{12}$$

Hence we have to find $\vec{F}$ and $\vec{\rho}$, so that:

$$2c_i F_{x,i} + \rho_x - y_i \rho_z = 0 \tag{13a}$$

$$2c_i F_{y,i} + \rho_y + x_i \rho_z = 0 \tag{13b}$$

$$\sum_{i=1}^{N} F_{x,i} = F_{x,\text{req}} \tag{13c}$$

$$\sum_{i=1}^{N} F_{y,i} = F_{y,\text{req}} \tag{13d}$$

$$\sum_{i=1}^{N} (x_i F_{y,i} - y_i F_{x,i}) = M_{z,\text{req}} \tag{13e}$$

This linear system of equations can be written as

$$A\vec{x} = \vec{b} \quad \Leftrightarrow \quad \vec{x} = A^{-1}\vec{b} \tag{14}$$

where the system matrix, the solution vector and the right-hand side vector are given by

$$A = \begin{bmatrix} C^{(2)} & R^T \\ R & 0_{3,3} \end{bmatrix} \;,\; \vec{x} = \begin{bmatrix} \vec{F} \\ \vec{\rho} \end{bmatrix} \;,\; \vec{b} = \begin{bmatrix} 0_{2N,1} \\ \vec{F}_{\text{req}} \end{bmatrix} \tag{15}$$

where $0_{m,n}$ is a zero sub-matrix with m rows and n columns, $C^{(2)}$ is the Hessian sub-matrix of the approximate power $P^{(2)}$ with size $2N \times 2N$ and R is the requirement constraints sub-matrix with size $3 \times 2N$.

Exact solution without constraints

We are looking for a method to correct the solution found from (14-15) and find a better minimization of the power computed in the exact way, i.e. with $m = 3/2$. To this end, we use the Newton-Raphson method [5]:

We consider the problem $L(x) = 0$, for which an approximate solution x_0 could be determined using an approximate expression of L. We will approach the function L to first order (in one dimension we can say that we consider L almost equal to its tangent at that point, as shown in Figure 2):

$$L(x) \approx L(x_0) + L'(x_0)(x - x_0) \tag{16a}$$

A better approximation x_1 is then obtained by solving

$$0 = L(x_0) + L'(x_0)(x_1 - x_0) \tag{16b}$$

This leads to the following iterative process:

$$x_{n+1} = x_n - \frac{L(x_n)}{L'(x_n)} \tag{16c}$$

The monotony of L guarantees the convergence.

Applying this method to

$$\vec{L} = \nabla P^{(3/2)} \tag{17}$$

we have to solve

$$C^{(3/2)}(\vec{F}^{(k)})\vec{F}^{(k+1)} = C^{(3/2)}(\vec{F}^{(k)})\vec{F}^{(k)} - \nabla P^{(3/2)}(\vec{F}^{(k)}) \tag{18}$$

where $C^{(3/2)}$ is the Hessian matrix of $P^{(3/2)}$.

Starting from the solution $\vec{F}_0$ of the problem (14-15), the iterative process is then:

$$\begin{bmatrix} C^{(3/2)}(\vec{F}^{(k)}) & R^T \\ R & 0_{3,3} \end{bmatrix} \begin{bmatrix} \vec{F}^{(k+1)} \\ \vec{\rho} \end{bmatrix} = \begin{bmatrix} C^{(3/2)}(\vec{F}^{(k)})\vec{F}^{(k)} - \nabla P^{(3/2)}(\vec{F}^{(k)}) \\ \vec{F}_{\text{req}} \end{bmatrix} \tag{19}$$

Exact solution with constraints

Taking into account the maximum thrust constraint, the approximate Lagrangian becomes:

$$\Lambda^{(2)}(\vec{F}, \vec{\rho}, \vec{\mu}) \equiv P^{(2)}_{\text{tot}}(\vec{F}) - \vec{\rho} \cdot \vec{R}(\vec{F}) - \vec{\mu} \cdot \vec{M}(\vec{F}) \tag{20}$$

and (12) is supplemented with

$$\nabla_{\vec{\mu}} \Lambda^{(2)} = \vec{0} \tag{21}$$

Hence (13a) and (13b) become:

$$2c_i F_{x,i} + \rho_x - y_i \rho_z + 2\mu_i F_{x,i} = 0 \tag{22a}$$
$$2c_i F_{y,i} + \rho_y + x_i \rho_z + 2\mu_i F_{y,i} = 0 \tag{22b}$$

The gradient with respect to $\vec{\rho}$ does not change, hence (13c-e) still hold. The vanishing of the gradient with respect to $\vec{\mu}$ yields:

$$F_{x,i}^2 + F_{y,i}^2 = T_{\max,i}^2 \tag{23}$$

These equations are non-linear in $\vec{F}$, and this prevents us from implementing directly the maximum thrust constraint in the minimization algorithm : we need to have a first evaluation of $\vec{F}$ to be able to implement (an approximation of) the constraint in a linear way. To handle the actuators limitations we define a subset J listing all indices i corresponding to saturated thrusters. The equations for the maximum thrust constraint of those actuators will then be added in the problem. The resulting set of equations can be written again as in (14), where

$$A = \begin{bmatrix} C^{(2)} & R^T & M^T(\vec{F}_0) \\ R & 0_{3,3} & 0_{3,N(J)} \\ M(\vec{F}_0) & 0_{N(J),3} & 0_{N(J),N(J)} \end{bmatrix}, \vec{x} = \begin{bmatrix} \vec{F} \\ \vec{\rho} \\ \vec{\mu} \end{bmatrix}, \vec{b} = \begin{bmatrix} 0_{2N,1} \\ \vec{F}_{\text{req}} \\ \vec{D}(\vec{F}_0) \end{bmatrix} \tag{24}$$

where M is a $N(J) \times 2N$ matrix and $\vec{D}\ \vec{F}_0$ is a $N(J) \times 1$ vector, where $N(J)$ is the number of indices in J. In the initial step, we take J empty, that is to say that we solve (14-15). We obtain an initial allocation $\vec{F}_0$ that takes no limitations into account. This initial allocation is then used to start the iteration process: we compute for each actuator

$$T_{\max,i}(\alpha_i) = T_{\max,i}(\arctan(F_{y,i} / F_{x,i})) \tag{25}$$

If the azimuth α_i is in the forbidden zone, we take the closest azimuth allowed (on the edge of the forbidden zone), say α_i^*, and set:

$$F_{x,i}^* = T_i^{(\text{old})} \cos \alpha_i^* \quad \text{and} \quad F_{y,i}^* = T_i^{(\text{old})} \sin \alpha_i^* \tag{26}$$

Indeed, even if the azimuth is forbidden, the thrust allocated to this thruster might be low. Therefore, we prefer to keep its value, and to construct the matrix M and corresponding entries in the right-hand side vector we would rather use the equation

$$2F_{x,i}^* F_{x,i} + 2F_{y,i}^* F_{y,i} = (F_{x,i}^*)^2 + (F_{y,i}^*)^2 + (T_i^*)^2 \tag{27}$$

This defines both M and $\vec{D}\ \vec{F}_0$ and will keep the azimuth angle α_i fixed. Note that by setting the azimuth to the closest edge of the forbidden zone, we risk to have a swap from one edge to the other over the time steps. To avoid this, we keep in memory the previous time step azimuth and if it is already on the edge of the forbidden zone, we will choose the same edge. If the constraint (10) is violated, we set $\vec{F}_i^{(\text{new})}$ so that

$$\vec{F}_i^{(\text{new})} = \frac{T_{\max,i}(\alpha_i)}{T_i^{(\text{old})}} \vec{F}_i^{(\text{old})} \tag{28}$$

In both cases, the index i is added to J, and we iterate the process with a non-empty matrix M this time. The iteration stops when J does not change any more, which at least happens when all the actuators are saturated. Sometimes it will then not be possible to match the required forces.

Starting from the solution of (14, 24), Newton's method is used as in (18), and leads to solve:

$$\begin{bmatrix} C^{(3/2)}(\vec{F}^{(k)}) & R^T & M^T(\vec{F}_0) \\ R & 0_{3,3} & 0 \\ M(\vec{F}_0) & 0 & 0 \end{bmatrix} \begin{bmatrix} \vec{F}^{(k+1)} \\ \vec{\rho} \\ \vec{\mu} \end{bmatrix} = \begin{bmatrix} C^{(3/2)}(\vec{F}^{(k)})\vec{F}^{(k)} - \nabla P^{(3/2)}(\vec{F}^{(k)}) \\ \vec{F}_{\text{req}} \\ D(\vec{F}_0) \end{bmatrix} \tag{29}$$

At the end of the iterative process, we obtain an allocation of forces that minimizes the power computed in the exact way, respects the actuators and matches the required forces in the best achievable way.

RESULTS

The test configuration consists of 4 starboard thrusters and 4 port side thrusters, see Figure 3 for an outline and Table 1 for the main dimensions and the thruster characteristics.

The required surge and sway forces and yaw moment that we use as input for the allocation algorithm are taken from a model test and have been filtered to take out the wave frequency variations. The required forces do not represent any specific environment, but are the output signals of the DP systems controller, see Figure 1. The results correspond to simulations for a 5 minutes time interval. Note, however, that each time step is solved independently from the others. To demonstrate the interest of the re-allocation in the '*J*-loop', we first present – for reference purposes – the results obtained by solving the allocation problem without limitations for the thrust and azimuth. As can be seen from Figure 4, the solutions match exactly the required forces (with a relative error < 10^{-15}). However, the allocation algorithm asks some thrusters to perform beyond their maximum thrust, as shown in Figure 5. If we truncate these thrust values, then the total forces and moment are quite different from the required values, see Figure 6. It is noted that this is a quite crude method to deal with thruster saturation and that allocation algorithms in real-life DP systems will probably use a more advanced approach.

Figures 7 and 8 demonstrate the effect of the '*J*-loop'. The allocation algorithm now accounts for the maximum thrust and forbidden zone restrictions immediately. It re-distributes the extra forces left by the truncation of the thrust of PS1 and PS2 to the other thrusters: we see that now at some point the other thrusters reach their maximum capacity too. When all thrusters are saturated, the required forces may not be exactly matched, but the accuracy is still satisfactory (relative error < 10^{-3}).

CONCLUSIONS AND RECOMMENDATIONS

Based on the results of the comparison between the existing Lagrange allocation method and the improved method described in this paper, the following conclusions were drawn.

1. We have developed a method to solve the thruster allocation with minimization of the exact power. The use of the Newton-Raphson method is to be recommended: depending on the configuration, it may lead to significant power (energy) savings and there are no drawbacks to its use (no loss of accuracy, satisfying computation time).
2. An iterative process has also been studied to take the actuators limitations into account. This process includes some subtle points about the way to handle the forbidden zone of the azimuthing thrusters, which make the algorithm time-dependent. The algorithm can handle all types of thrusters
3. This results in a very well-balanced allocation with a sound mathematical-physical basis: it both matches the requirements and it respects the limitations of the actuators.

However, some improvements may still be made. Here we give some suggestions that may be interesting to explore in the future.

When the minimization algorithm fails

As we have shown previously, by adding equations to the minimization problem we may arrive to a point where the system has no solution:

- Either the 3 equations for forces and moment requirements, combined with the maximum thrust constraints equations, fully determine the allocation. This happens with very simple configurations, but is very rare with more complex configurations: in complex configurations, there are a lot of degrees of freedom, and there will be different possibilities to meet the requirements (when it is possible). In these cases, we need to add equations to choose one possibility: that is the role of the energy minimization.
- Or the total thrust required is too high, and due to the actuators limitations it will not be possible to reach it: the allocation problem has no solution.

To handle these situations (which are pointed out by the nullity of the system matrix determinant), we suggest:

- First, try to solve the linear system obtained from the forces and moment requirements and actuators limitations. This will give the only solution of the allocation problem if it exists. As it happens only for very simple and unrealistic configurations, this has not been implemented yet.
- Then, if it appears that the requirements cannot be met, we should look for a compromise. As a matter of fact, we cannot just set automatically all the actuators to their

maximum thrust value, because it may lead to a global yaw moment very different from the required one. For the moment, we compare the accuracy of the different allocations in the '*J*-loop' in terms of yaw moment, and choose the best one. This is a way to find a compromise, but it might be done in a more systematic and accurate way, for instance by using a penalty function.

Time step dependency

The results presented above are computed for an input of 5 minutes, but each time step is taken independently. In reality, the actuators cannot change their RPM and azimuth instantly, and given the RPM and azimuth at time step k, it may be impossible to reach the RPM and azimuth that the allocation request at time step $k+1$: the time interval will not be sufficient, and the actuator will only reach in-between values. The effective total forces and moment could then be different from the required forces and moment, because the thrusters are lagging behind. This typically happens in relatively severe environments, close to the limitations of the vessel's stationkeeping capabilities. In mild environments, the thrusters will generally be capable of delivering the requested RPMs and azimuth angles.

TABLES AND FIGURES

Table 1: Test configuration main dimensions and thruster characteristics.

Description	**Value**
Length of pontoon	97.50 m
Width of pontoon	23.20 m
Distance between pontoons	32.80m
Maximum thrust	496 kN
Maximum power	3000 kW

Figure 1: Schematic overview of a DP system.

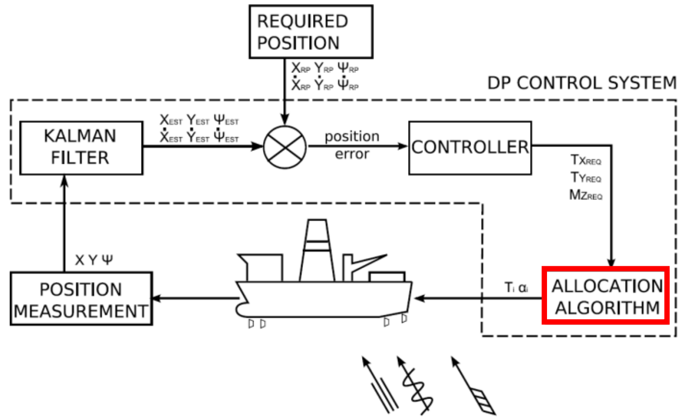

Figure 2: Schematical representation of Newton's method. Red curve indicates exact function, blue and green curves indicate successive linear (tangent) approximations.

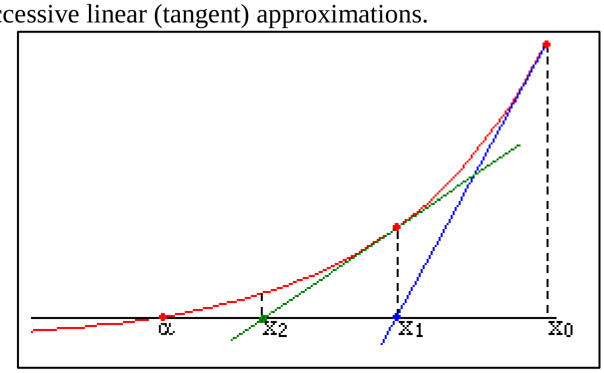

Figure 3: Test configuration with 8 azimuthing thrusters: 4 on the portside floater (PS1, PS2, PS3 and PS4) and 4 on the starboard floater (SB1, SB2, SB3 and SB4). The forbidden zones are indicated as grey sectors.

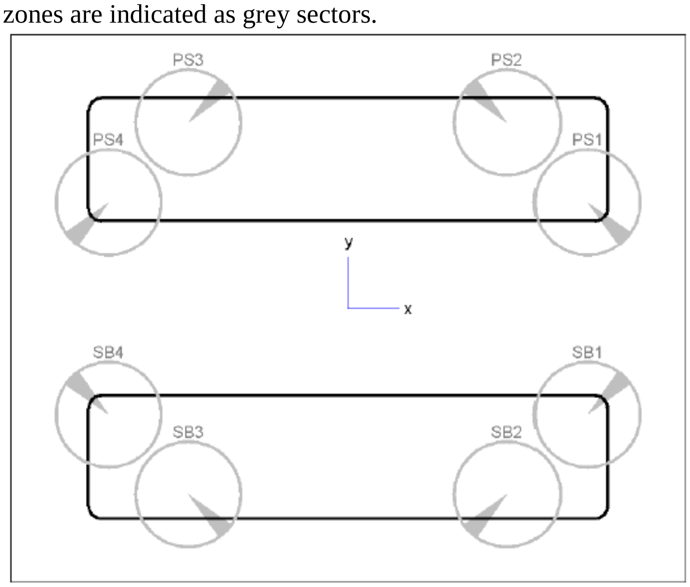

Figure 4: Results for test configuration without limitations on thrust and azimuth; total surge force (top left), sway force (middle left), yaw moment (bottom left), thrust (top right), azimuth (middle right) and power (bottom right); green line = approximate solution (a), blue line = exact solution (b), red line = required values (req).

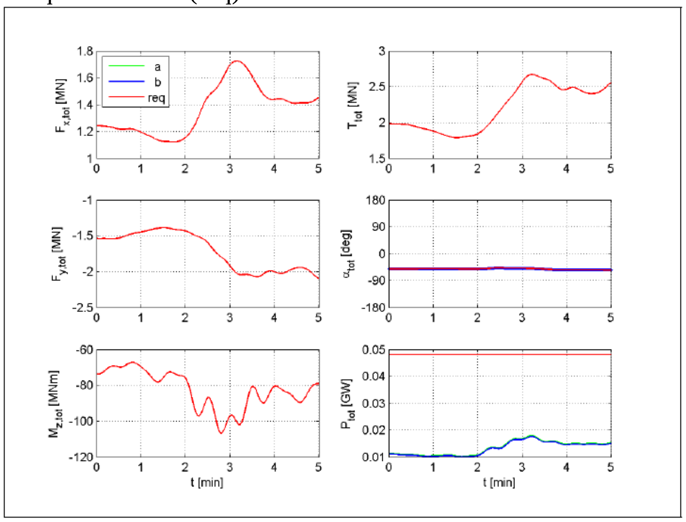

Figure 5: Results for test configuration without limitations on thrust and azimuth; thrust (left) and azimuth (right) of portside thrusters PS1-PS4; green line = approximate solution (a), blue line = exact solution (b), red line = maximum thrust, red bar = forbidden zone.

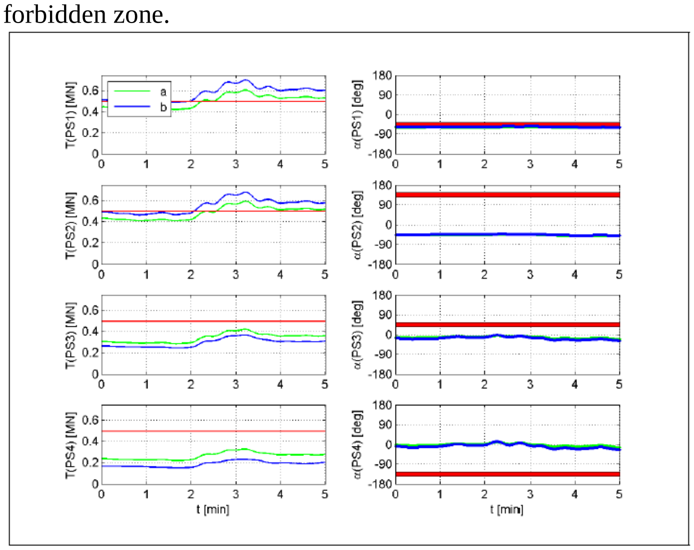

Figure 6: Results for test configuration with limitations on thrust applied a posteriori; total surge force (top left), sway force (middle left), yaw moment (bottom left), thrust (top right), azimuth (middle right) and power (bottom right); green line = approximate solution (a), blue line = exact solution (b), red line = required values (req).

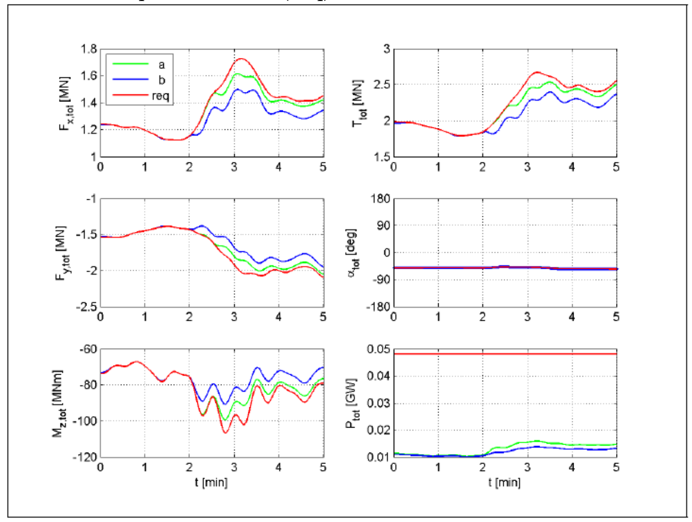

Figure 7: Results for test configuration with limitations on thrust and azimuth accounted for directly in optimization algorithm; total surge force (top left), sway force (middle left), yaw moment (bottom left), thrust (top right), azimuth (middle right) and power (bottom right); green line = approximate solution (a), blue line = exact solution (b), red line = required values (req).

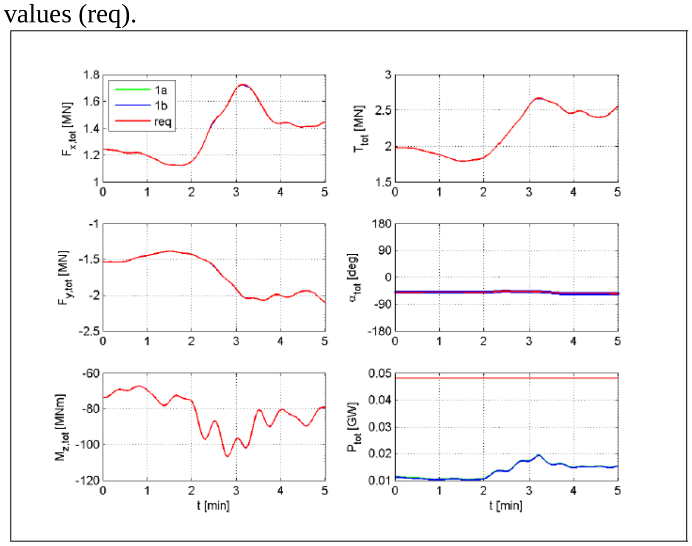

Figure 8: Results for test configuration with limitations on thrust and azimuth accounted for directly in optimization algorithm; thrust (left) and azimuth (right) of portside thrusters PS1-PS4; green line = approximate solution (a), blue line = exact solution (b), red line = maximum thrust, red bar = forbidden zone.

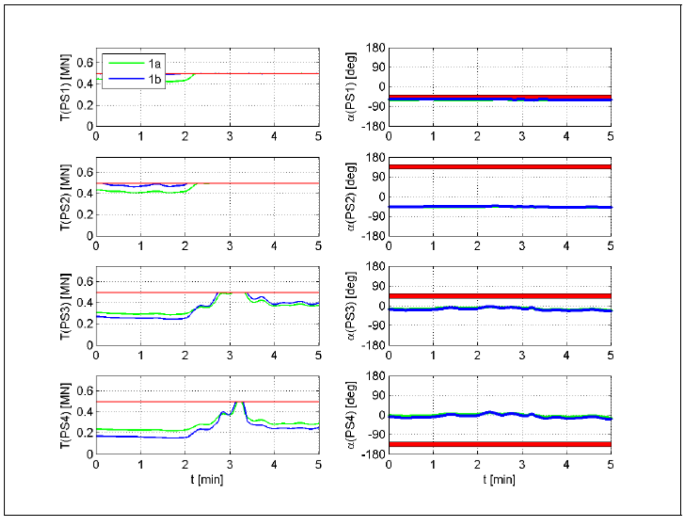

REFERENCES

[1] Serraris, J.J., (MARIN), "*Time-domain Analysis for DP Simulations*", OMAE2009-79587, OMAE Conference, Honolulu, 2009.

[2] Aalbers, A.B., Jansen, R.B.H.J., Kuipers, R.J.P.E. and van Walree, R., "*Developments in dynamic positioning systems for offshore stationkeeping and offloading*", OMAE Conference, Copenhagen, 1995.

[3] Aalbers, A.B. (MARIN) and Merchant, A.A. (Keppel-FELS), "*The Hydrodynamic Model Testing for Closed Loop DP Assisted Mooring*", OTC1996-8261, Offshore Technology Conference, Houston, 1996.

[4] Van Dijk, R.R.T. and Aalbers, A.B. (MARIN), "*What Happens in Water - The use of Hydrodynamics to Improve DP*", MTS Dynamic Positioning Conference, Houston, 2001.

[5] Hildebrand, F.B., *Introduction to Numerical Analysis*, 2nd edition, Dover Books on Advanced Mathematics, 1987.